

A Review of CP Violation Measurements in Charm at LHCb

Federico Betti[†]

*CERN (European Organization for Nuclear Research)
Espl. des Particules 1, 1211 Meyrin, Switzerland*

Abstract

The LHCb experiment has been able to collect the largest sample ever produced of charm-hadron decays, performing a number of measurements of observables related to CP violation in the charm sector. In this document, the most recent results from LHCb on the search of direct CP violation in $D^0 \rightarrow K_s^0 K_s^0$, $D_{(s)}^+ \rightarrow h^+ \pi^0$ and $D_{(s)}^+ \rightarrow h^+ \eta$ decays are summarised, in addition to the most precise measurement of time-dependent CP asymmetry in $D^0 \rightarrow h^+ h^-$ decays and the first observation of mass difference between neutral charm-meson eigenstates.

Published in *Symmetry* **13** (2021) 8, 1482

[†]federico.betti@cern.ch

1 Introduction

For a generic hadron M and its CP conjugate \bar{M} , the following decay amplitudes in the final state f and its CP conjugate \bar{f} are defined

$$A_f = \langle f | \mathcal{H} | M \rangle, \quad \bar{A}_{\bar{f}} = \langle \bar{f} | \mathcal{H} | \bar{M} \rangle, \quad (1)$$

where \mathcal{H} is the effective decay Hamiltonian. The CP asymmetry of the decay $M \rightarrow f$ is therefore defined as

$$\mathcal{A}_{CP}(M \rightarrow f) \equiv \frac{\Gamma(M \rightarrow f) - \Gamma(\bar{M} \rightarrow \bar{f})}{\Gamma(M \rightarrow f) + \Gamma(\bar{M} \rightarrow \bar{f})} = \frac{1 - |\bar{A}_{\bar{f}}/A_f|^2}{1 + |\bar{A}_{\bar{f}}/A_f|^2}. \quad (2)$$

Direct CP violation, or CP violation in the decay, takes place when $|\bar{A}_{\bar{f}}|^2 \neq |A_f|^2$. For neutral mesons such as D^0 , mixing must be taken into account. The eigenstates $|D_H\rangle$ and $|D_L\rangle$ of the effective Hamiltonian, which have defined masses (m_H and m_L) and decay widths (Γ_H and Γ_L), can be written as a superposition of flavour eigenstates

$$|D_H\rangle = p|D^0\rangle - q|\bar{D}^0\rangle, \quad (3)$$

$$|D_L\rangle = p|D^0\rangle + q|\bar{D}^0\rangle, \quad (4)$$

where p and q are complex with $|p|^2 + |q|^2 = 1$. The mixing is described by the parameters

$$x \equiv \frac{m_H - m_L}{\Gamma}, \quad (5)$$

$$y \equiv \frac{\Gamma_H - \Gamma_L}{2\Gamma}, \quad (6)$$

with $\Gamma = (\Gamma_H + \Gamma_L)/2$. If $|q/p| \neq 1$, CP violation in the mixing occurs, and the probability of the D^0 meson to oscillate after a time t into \bar{D}^0 is different from that of the CP -conjugate process. If $f = \bar{f}$ and the phase

$$\phi_f \equiv \arg\left(\frac{q\bar{A}_f}{pA_f}\right) \quad (7)$$

is different from 0, CP violation manifests in the interference between mixing and decay. The time-dependent CP asymmetry between the probability of an initially pure D^0 meson and an initially pure \bar{D}^0 meson to decay into the final state f after a time t

$$\mathcal{A}_{CP}(D^0(t) \rightarrow f) \equiv \frac{\Gamma(D^0(t) \rightarrow f) - \Gamma(\bar{D}^0(t) \rightarrow f)}{\Gamma(D^0(t) \rightarrow f) + \Gamma(\bar{D}^0(t) \rightarrow f)} \quad (8)$$

is different from 0 if CP violation occurs either in the mixing or in the interference between mixing and decay. In the D^0 meson system, the time-dependent CP asymmetry can be written as

$$\mathcal{A}_{CP}(D^0(t) \rightarrow f) \approx a_f^d + \frac{4|A_f|^2|\bar{A}_f|^2}{(|A_f|^2 + |\bar{A}_f|^2)^2} \Delta Y_f \frac{t}{\tau_{D^0}}, \quad (9)$$

where a_f^d is equal to the direct CP asymmetry, τ_{D^0} is the D^0 lifetime and ΔY_f , the observable describing the amount of time-dependent CP violation, is defined according to

the “theoretical” parametrisation introduced in Refs. [1, 2]. The coefficient in front of ΔY_f differs from unity by approximately $\mathcal{O}(10^{-6})$, resulting in ΔY_f to be equal to the slope of $\mathcal{A}_{CP}(D^0(t) \rightarrow f)$.

The combination of Cabibbo–Kobayashi–Maskawa matrix elements responsible for CP violation in charm decays is $\text{Im}(V_{cb}V_{ub}^*/V_{cs}V_{us}^*) \simeq -6 \times 10^{-4}$, resulting in asymmetries typically of the order of 10^{-4} – 10^{-3} in the Standard Model (SM). Due to the presence of low-energy strong-interaction effects, theoretical predictions are difficult to compute reliably [3–20]. Some calculations are performed using dynamical methods of QCD, such as Light-Cone Sum Rules [8, 10, 19]. Other studies rely on perturbative parameterisations of the branching fractions and the CP asymmetries as a function of the topological amplitudes contributing to the dominant and subleading amplitudes in $SU(3)_F$ or U -spin breaking, fitting them to the measured values [3, 4, 11–16, 18, 20].

Almost all the measurements of CP violation in charm hadrons have been performed at the B -factories Belle and BaBar and at the hadron-collider experiments LHCb and CDF. The production cross-section of charm in proton–proton (pp) (or proton–antiproton) collisions is much larger than that at the B -factories, for example $\sigma(pp \rightarrow c\bar{c}X) = (2369 \pm 12) \mu\text{b}$ at $\sqrt{s} = 13$ TeV in the LHCb acceptance [21], whereas $\sigma(e^+e^- \rightarrow \gamma^* \rightarrow c\bar{c}) = 1.3$ nb at $\sqrt{s} = 10.58$ GeV. Despite the large hadronic background, not present in the low-multiplicity environment of the e^+e^- machines, LHCb was therefore able to collect the largest sample ever produced of charm-hadron decays, performing a number of measurements of observables related to CP violation in the charm sector, such as: searches for direct CP asymmetry in $D_{(s)}^+$ decays [22–24]; time-dependent CP violation in singly Cabibbo suppressed (SCS) D^0 decays [25–28]; direct CP asymmetries in SCS D^0 decays [29–31]; CP violation in mixing using $D^0 \rightarrow K^+\pi^-$ decays [32, 33]; CP violation in multi-body D^0 decays [34–39]; CP violation in D^0 decays into final states with K_s^0 [40, 41]; and CP violation in baryon decays [42, 43]. The measurement of $\Delta\mathcal{A}_{CP} \equiv \mathcal{A}_{CP}(D^0 \rightarrow K^+K^-) - \mathcal{A}_{CP}(D^0 \rightarrow \pi^+\pi^-)$ with the full data sample collected by the LHCb detector led to the first observation of CP violation in the decay of charm hadrons [44]. The result, that challenges perturbative and sum-rule estimates of $\Delta\mathcal{A}_{CP}$ [19, 45], prompted a renewed interest of the theory community in the field, sparking a discussion whether the signal is consistent with the Standard Model or if it is a sign of new physics [46–56]. While according to some studies the discrepancy is due to an enhancement of rescattering beyond expectation [12–14, 16, 18, 47, 49], for other authors the reason of the discrepancy must be found in new interactions beyond the SM [46]. Possible contributions of new physics to $\Delta\mathcal{A}_{CP}$, such as models involving Z' , have been studied [46, 51, 53].

Additional investigations are therefore crucial to clarify the picture and solve open theoretical puzzles. More precise measurements of branching fractions and CP asymmetries will allow the sum rules relating the CP asymmetries of different decay channels to be tested, and a better precision on the predictions obtained with the topological amplitudes to be reached [16, 18, 48, 50].

In the following Section, the most recent results obtained by the LHCb collaboration in the field of CP violation in charm will be summarised, namely the measurements of: CP asymmetry in $D^0 \rightarrow K_s^0 K_s^0$ decays; CP asymmetry in $D_{(s)}^+ \rightarrow h^+\pi^0$ and $D_{(s)}^+ \rightarrow h^+\eta$ decays, where h^+ denotes a π^+ or K^+ meson; ΔY in $D^0 \rightarrow K^+K^-$ and $D^0 \rightarrow \pi^+\pi^-$ decays; and mixing parameters by using $D^0 \rightarrow K_s^0\pi^+\pi^-$ decays. In Section 3, the conclusions and the prospects for future measurements of CP violation in charm at LHCb are given.

2 Recent results from LHCb

The LHCb detector [57, 58] is a single-arm forward spectrometer that covers the pseudorapidity range between 2 and 5, whose main goal is the study of particles containing b or c quarks. The tracking system consists of a silicon-strip vertex detector (VELO), a large-area silicon-strip detector, a dipole magnet and three stations of silicon-strip detectors and straw drift tubes. The momentum of charged particles is measured with a relative uncertainty varying from 0.5% to 1.0%. The impact parameter (IP) of a track, defined as its minimum distance to a primary pp collision vertex (PV), is measured with a resolution of $(15 \pm 29/p_T)$ μm , where p_T is the momentum transverse to the beam, expressed in GeV/c . Particle identification of charged hadrons is performed using information from two ring-imaging Cherenkov detectors. Electrons, photons and hadrons are identified by a calorimeter system made of scintillating-pad and preshower detectors, an electromagnetic and a hadronic calorimeter. Muons are identified by a system composed of alternating layers of iron and multiwire proportional chambers. The online event selection is performed by a trigger, which consists of a hardware stage followed by a software stage. The hardware stage is based on information from the calorimeter and muon systems, whereas the software stage applies a full event reconstruction.

In the measurements of CP asymmetries in the decays of neutral D^0 mesons to CP eigenstates, the D^0 flavour, when produced, is determined by the charge of the accompanying “tagging” pion in the strong $D^{*+} \rightarrow D^0\pi^+$ (Inclusion of the charge-conjugate process is implied throughout this document unless explicitly specified.) decay promptly produced in the pp collisions, or by the charge of the muon in the semileptonic b -hadron secondary decays. Due to the higher production cross section of charm with respect to that of beauty, the data samples selected with prompt tag usually convey a signal yield which is a factor ~ 5 larger than that with semileptonic tag.

The “raw” asymmetry obtained by counting the positively- and negatively-tagged signal candidates is not equal to the physical asymmetry \mathcal{A}_{CP} , but it includes also experimental effects due to production asymmetry \mathcal{A}_P and detection asymmetry \mathcal{A}_D . The production asymmetry is due to different production rates of the charm meson and its anti-meson, whereas different interaction cross-sections of particle and antiparticles with the detector, which is not perfectly symmetric, result in the detection asymmetry. These nuisance asymmetries, averaged over phase space for selected events, are usually $\mathcal{O}(10^{-2})$ or less [59–62], allowing the measured raw asymmetry \mathcal{A}_{raw} to be written as a sum of the physical and the experimental asymmetries. For example, the raw asymmetry of promptly-tagged D^0 mesons that decay in a CP eigenstate f can be approximated as

$$\mathcal{A}_{\text{raw}}(D^0 \rightarrow f) \approx \mathcal{A}_{CP}(D^0 \rightarrow f) + \mathcal{A}_P(D^{*+}) + \mathcal{A}_D(\pi^+), \quad (10)$$

where $\mathcal{A}_P(D^{*+})$ is the production asymmetry of the D^{*+} meson and $\mathcal{A}_D(\pi^+)$ is the detection asymmetry of the tagging pion. The approximation is valid up to corrections of $\mathcal{O}(10^{-6})$. Calibration samples which share the same production and detection asymmetries of the signal sample are typically used to cancel the nuisance asymmetries and obtain the CP asymmetry.

2.1 Measurement of CP asymmetry in $D^0 \rightarrow K_s^0 K_s^0$ decays

In the $D^0 \rightarrow K_s^0 K_s^0$ decay, the only contributing amplitudes proceed via tree-level exchange and loop-suppressed diagrams which are of similar size and vanish in the flavour-SU(3) limit. Their interference could result in a CP asymmetry up to the percent level in the SM [63]. The CLEO, Belle and LHCb (with data collected during the LHC Run 1) collaborations have measured in the past the CP asymmetry $\mathcal{A}_{CP}(D^0 \rightarrow K_s^0 K_s^0)$ [64–66], with the best precision reached by Belle, at the level of 1.5%. The update performed by LHCb with data collected during the LHC Run 2, corresponding to an integrated luminosity of 6 fb^{-1} , is reported here.

From an experimental point of view, the relatively large lifetime of K_s^0 meson is challenging, because the majority of K_s^0 mesons decay after the LHCb Vertex Locator and their decay products can be reconstructed only in the tracking stations further downstream along the beam axis. The first software trigger stage is designed to accept the K_s^0 mesons whose pions are reconstructed also in the Vertex Locator (referred to as “long” and indicated by “L” in the following), resulting in a worse trigger efficiency for K_s^0 whose pions are reconstructed only in the downstream part of the tracking system (referred to as “D”). Depending on how the decay products of the two K_s^0 mesons are reconstructed, the data sample is split in three categories that are analysed separately: two long (LL), one long and one downstream (LD) and two downstream (DD) K_s^0 mesons. Once the two K_s^0 mesons are combined in a D^0 candidate, its flavour is determined by looking at the charge of the accompanying pion in the reconstructed strong decay $D^{*+} \rightarrow D^0 \pi^+$. The data sample is further split in two categories, according to whether the D^{*+} candidate is compatible or incompatible with having originated from the PV. The PV compatibility classification is not performed for the DD sample, because of its low statistics and signal purity. A multivariate classifier sensitive to the signal-to-background ratio is used to select high signal purity D^{*+} candidates. Finally, data collected in 2015 and 2016 are analysed separately from those collected in 2017–2018, because of differences in trigger requirements between these two periods.

In order to measure the raw asymmetry of the signal, an unbinned maximum-likelihood fit is performed to the joint distribution of the invariant masses of the K_s^0 mesons and the difference $\Delta m \equiv m(K_s^0 K_s^0 \pi^+) - m(K_s^0 K_s^0)$, simultaneously to candidates of both flavours. The total probability density function is parameterised by the sum of the signal component, peaking in the three observables, and seven additional components, which describe different kinds of background. Fit projections on Δm distribution are reported in Figure 1, which shows how the mass resolution and the signal purity change between the different LL, LD and DD categories and between PV-compatible and PV-incompatible categories.

A data sample of reconstructed $D^{*+} \rightarrow D^0 (\rightarrow K^+ K^-) \pi^+$ decays, whose CP asymmetry is known to a precision much higher than that of the signal decay [31], is used as a calibration sample to correct for D^{*+} production asymmetry and π^+ detection asymmetry. As experimental asymmetries are a function of pion and D^{*+} kinematics, the kinematics of the calibration samples are weighted to match those of the signal by using a multivariate classifier. Various contributions to the systematic uncertainty are evaluated, namely related to weighting procedure, difference between signal and calibration modes and fit model.

All the results obtained in each subsample are statistically compatible with each other

and their combination gives:

$$\mathcal{A}_{CP}(D^0 \rightarrow K_s^0 K_s^0) = (-3.1 \pm 1.2 \pm 0.4 \pm 0.2)\%,$$

where the first uncertainty is statistical, the second systematic and the third is related to the knowledge of $\mathcal{A}_{CP}(D^0 \rightarrow K^+ K^-)$ [67]. This measurement, the most precise of this quantity to date, is in agreement with the previous determinations [64–66] and is compatible with no CP violation at the level of 2.4 standard deviations.

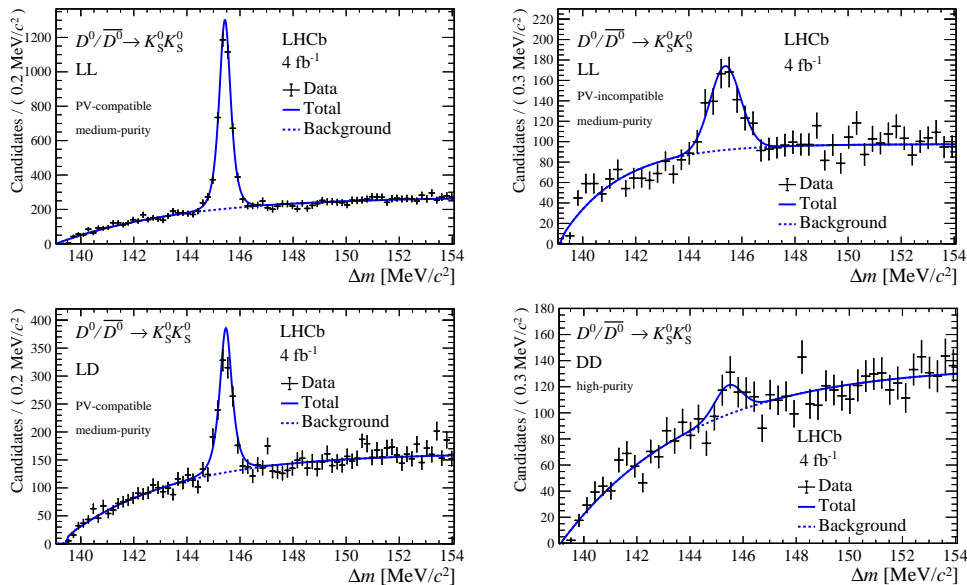


Figure 1: Distributions and fit projections of the Δm distribution for representative candidate categories (2017–2018 data sample).

2.2 Search for CP violation in $D_{(s)}^+ \rightarrow h^+ \pi^0$ and $D_{(s)}^+ \rightarrow h^+ \eta$ decays

The study of CP asymmetry in the two-body $D_{(s)}^+ \rightarrow h^+ \pi^0$ and $D_{(s)}^+ \rightarrow h^+ \eta$ decays provides interesting tests of the SM. In particular, SCS $D_s^+ \rightarrow K^+ \pi^0$, $D^+ \rightarrow \pi^+ \eta$ and $D_s^+ \rightarrow K^+ \eta$ decays receive contributions from two different weak phases allowing CP violation at tree-level, expected to be of the order of 10^{-3} – 10^{-4} according to the SM [8]. In the SM, the CP asymmetry of the SCS $D^+ \rightarrow \pi^+ \pi^0$ mode is expected to be zero as a result of isospin constraints [12, 17, 20, 53]. It is possible to define the isospin sum rule

$$R = \frac{\mathcal{A}_{CP}(D^0 \rightarrow \pi^+ \pi^-)}{1 + \frac{\tau_{D^0}}{\mathcal{B}_{+-}} \left(\frac{\mathcal{B}_{00}}{\tau_{D^0}} + \frac{2}{3} \frac{\mathcal{B}_{+0}}{\tau_{D^+}} \right)} + \frac{\mathcal{A}_{CP}(D^0 \rightarrow \pi^0 \pi^0)}{1 + \frac{\tau_{D^0}}{\mathcal{B}_{00}} \left(\frac{\mathcal{B}_{+-}}{\tau_{D^0}} + \frac{2}{3} \frac{\mathcal{B}_{+0}}{\tau_{D^+}} \right)} - \frac{\mathcal{A}_{CP}(D^+ \rightarrow \pi^+ \pi^0)}{1 + \frac{3}{2} \frac{\tau_{D^+}}{\mathcal{B}_{+0}} \left(\frac{\mathcal{B}_{00}}{\tau_{D^0}} + \frac{\mathcal{B}_{+-}}{\tau_{D^0}} \right)}, \quad (11)$$

where τ_D^+ and τ_D^0 represent the D^+ and D^0 lifetimes and \mathcal{B}_{+-} , \mathcal{B}_{00} and \mathcal{B}_{+0} are the branching fractions of the $D^0 \rightarrow \pi^+ \pi^-$, $D^0 \rightarrow \pi^0 \pi^0$ and $D^+ \rightarrow \pi^+ \pi^0$ decays, respectively. A non-zero value of $\mathcal{A}_{CP}(D^+ \rightarrow \pi^+ \pi^0)$, associated with a verification that R is consistent with 0, would represent a signal of new physics.

The Belle collaboration has reported the measurement of $\mathcal{A}_{CP}(D^+ \rightarrow \pi^+ \pi^0) = (2.31 \pm 1.24 \pm 0.23)\%$, corresponding to $R = (-2.2 + 2.7) \times 10^{-3}$ [68], and, more recently, precise

measurements of $\mathcal{A}_{CP}(D_s^+ \rightarrow K^+\pi^0)$, $\mathcal{A}_{CP}(D_s^+ \rightarrow \pi^+\eta)$ and $\mathcal{A}_{CP}(D_s^+ \rightarrow K^+\eta)$ with uncertainties ranging from 0.4% to 4.5% [69]. The measurements of the CP asymmetries in the $D_{(s)}^+ \rightarrow h^+\pi^0$ and $D_{(s)}^+ \rightarrow h^+\eta$ decays (except for $D_s^+ \rightarrow \pi^+\pi^0$, that proceeds via an annihilation topology decay and is therefore highly suppressed) performed by LHCb with an integrated luminosity of 9 fb^{-1} and 6 fb^{-1} , respectively, are summarised here.

The π^0 and η mesons are reconstructed in the $e^+e^-\gamma$ final state, which allows the secondary decay vertex to be reconstructed, suppressing background originating from the pp collisions. This final state receives contributions from the $\pi^0 \rightarrow \gamma\gamma$ and $\eta \rightarrow \gamma\gamma$ decays, where one photon is converted to an e^+e^- pair after interacting with the detector material, and the suppressed Dalitz $\pi^0 \rightarrow e^+e^-\gamma$ and $\eta \rightarrow e^+e^-\gamma$ decays. During the signal reconstruction process, a bremsstrahlung-recovery algorithm associates additional deposits from soft photons to those produced by the electrons in the electromagnetic calorimeter. Decays with a total of either zero or one bremsstrahlung photon per e^+e^- pair are selected. After the full selection is applied, about 86% of signal decays are found to be due to photon conversions, and the remaining part to the Dalitz decays.

The raw asymmetries are measured by means of two-dimensional extended simultaneous unbinned maximum-likelihood fits to the invariant mass $m(e^+e^-\gamma)$ and the invariant mass difference $m(h^+h^0) \equiv m(h^+e^+e^-\gamma) - m(e^+e^-\gamma) + M(h^0)$, where $M(h^0)$ is the known π^0 and η mass [70]. Two-dimensional probability density functions are used to model different contributions, namely signal decays, pure combinatorial background, combinatorial background due to real π^0 meson combined with an unrelated track, misidentification background and partially reconstructed low-mass background. The fits are performed simultaneously in categories depending on the running period, the number of recovered bremsstrahlung photons, the h^+ type (pion or kaon) and the candidate charge. The results of the fits are shown in Figures 2 and 3.

In order to cancel the production and detection asymmetries and obtain the CP asymmetries, a calibration sample of $D_{(s)}^+ \rightarrow K_s^0 h^+$ decays is used, after weighting its kinematic distributions to match those of the signal candidates. The values of $\mathcal{A}_{CP}(D_{(s)}^+ \rightarrow K_s^0 h^+)$ are known with sub-percent precision [24], significantly higher than the precision of this measurement. Systematic uncertainties related to the choice of the fit model, presence of $D_{(s)}^+$ candidates produced in secondary decays, different selection between signal and calibration sample, kinematic weighting and uncertainties of CP asymmetries of the calibration decays are evaluated.

The results are

$$\begin{aligned}\mathcal{A}_{CP}(D^+ \rightarrow \pi^+\pi^0) &= (-1.3 \pm 0.9 \pm 0.6)\%, \\ \mathcal{A}_{CP}(D^+ \rightarrow K^+\pi^0) &= (-3.2 \pm 4.7 \pm 2.1)\%, \\ \mathcal{A}_{CP}(D^+ \rightarrow \pi^+\eta) &= (-0.2 \pm 0.8 \pm 0.4)\%, \\ \mathcal{A}_{CP}(D^+ \rightarrow K^+\eta) &= (-6 \pm 10 \pm 4)\%, \\ \mathcal{A}_{CP}(D_s^+ \rightarrow K^+\pi^0) &= (-0.8 \pm 3.9 \pm 1.2)\%, \\ \mathcal{A}_{CP}(D_s^+ \rightarrow \pi^+\eta) &= (0.8 \pm 0.7 \pm 0.5)\%, \\ \mathcal{A}_{CP}(D_s^+ \rightarrow K^+\eta) &= (0.9 \pm 3.7 \pm 1.1)\%,\end{aligned}$$

where the first uncertainty is statistical and the second systematic [71]. All of the results are consistent with previous determinations [68, 69] and with no CP violation, and the first five constitute the most precise measurements to date of those observables. An average of

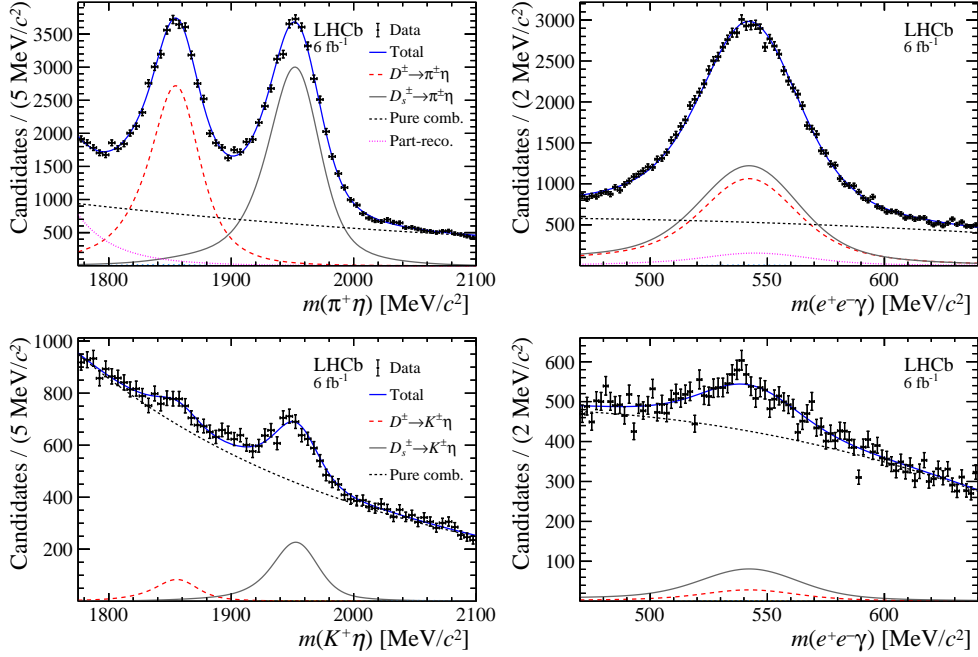


Figure 2: Distribution of (**left**) $m(h^+\eta)$ and (**right**) $m(e^+e^-\gamma)$ for (**top**) $D_{(s)}^+ \rightarrow \pi^+\eta$ and (**bottom**) $D_{(s)}^+ \rightarrow K^+\eta$ candidates, summed over all categories of the simultaneous fit, with projections of the fit result overlaid. $D^+ \rightarrow h^+\eta$ contribution is shown in dashed red, $D_s^+ \rightarrow h^+\eta$ in solid grey, pure combinatorial decays in dashed black and partially reconstructed background in dotted magenta. The misidentification background is too small to be seen.

$\mathcal{A}_{CP}(D^+ \rightarrow \pi^+\pi^0)$ between this result, the measurement by Belle [68] and a measurement by CLEO [72] gives $\mathcal{A}_{CP}(D^+ \rightarrow \pi^+\pi^0) = (0.43 \pm 0.79)\%$, corresponding to a value of $R = (0.1 \pm 2.4) \times 10^{-3}$, consistent with 0.

2.3 Search for time-dependent CP violation in $D^0 \rightarrow K^+K^-$ and $D^0 \rightarrow \pi^+\pi^-$ decays

The magnitude of the ΔY_f parameter is expected to be about 2×10^{-5} [56, 73]. The ΔY_f parameter is approximately equal, up to 1% relative corrections (For a detailed description of the theoretical parametrisation of mixing in D^0 decays, see Refs. [56, 74, 75]), to the negative of the parameter A_{Γ}^f that has been measured by the BaBar [76], CDF [77], Belle [78] and LHCb [25, 26, 28] collaborations, and the world average, assuming no difference is present between the K^+K^- and $\pi^+\pi^-$ final states, is $\Delta Y = (3.1 \pm 2.0) \times 10^{-4}$ [79]. The measurement of ΔY_f performed by LHCb with data collected during the LHC Run 2, corresponding to an integrated luminosity of 6 fb^{-1} , using $D^{*+} \rightarrow D^0\pi^+$ decays originated from primary pp interactions, is reported here.

Three decay modes are reconstructed: $D^0 \rightarrow K^+K^-$, $D^0 \rightarrow \pi^+\pi^-$ and $D^0 \rightarrow K^-\pi^+$, where the D^0 meson is associated with the accompanying pion in the $D^{*+} \rightarrow D^0\pi^+$ decay to determine its flavour when produced. The $D^0 \rightarrow K^-\pi^+$ mode has the same topology and kinematic distributions very similar to those of the signal channels and its CP asymmetry is known to be smaller than the current experimental uncertainty. For these reasons, the $D^0 \rightarrow K^-\pi^+$ mode is used as a control sample to develop and validate

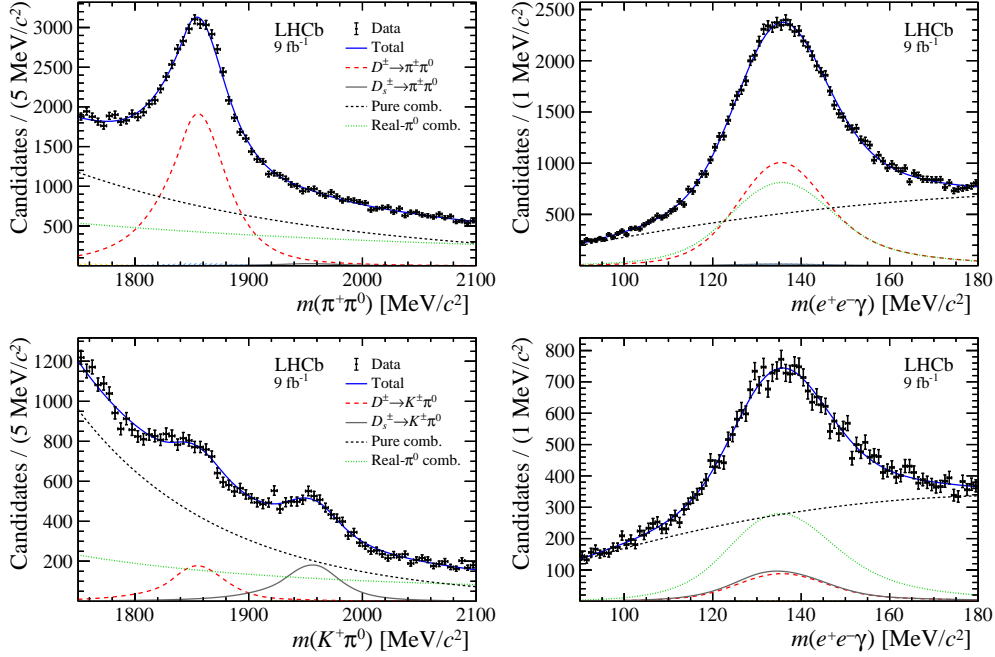


Figure 3: Distribution of (left) $m(h^+\pi^0)$ and (right) $m(e^+e^-\gamma)$ for (top) $D_{(s)}^+ \rightarrow \pi^+\pi^0$ and (bottom) $D_{(s)}^+ \rightarrow K^+\pi^0$ candidates, summed over all categories of the simultaneous fit, with projections of the fit result overlaid. $D^+ \rightarrow h^+\pi^0$ contribution is shown in dashed red, $D_s^+ \rightarrow h^+\pi^0$ in solid grey, pure combinatorial decays in dashed black and real- π^0 combinatorial background in dotted green. The misidentification background is too small to be seen.

the analysis. The data sample is divided in 21 intervals of D^0 decay times in the range of $(0.45-8) \tau_{D^0}$, where τ_{D^0} is the nominal D^0 lifetime [70]. In each decay time interval the signal yield is obtained by means of background subtraction in the $m(D^0\pi^+)$ distribution, where the signal window is defined as $[2009.2, 2011.3]$ MeV/ c^2 and the background candidates are taken from the lateral window $[2015, 2018]$ MeV/ c^2 . The weight assigned to the background candidates is determined with a binned maximum-likelihood fit to the $m(D^0\pi^+)$ distribution. The fit relies on an empirical model to describe the signal and the combinatorial background contributions. The $m(D^0\pi^+)$ distributions and the fit results are shown in Figure 4. After the full selection and background subtraction, the number of candidates in the signal region are 519, 58 and 18 millions for the $D^0 \rightarrow K^-\pi^+$, $D^0 \rightarrow K^+K^-$ and $D^0 \rightarrow \pi^+\pi^-$ decay channels, respectively. The candidates are split in subsamples according to year of data taking and magnet polarities. The analysis is performed on each subsample and the results are combined at the end.

In principle, the measurement of ΔY_f is insensitive to time-independent asymmetries such as the production and detection asymmetries, that depend only on the kinematics of the D^{*+} meson and the tagging pion. However, an indirect time dependence of the nuisance asymmetries exists because of the correlation between the kinematic variables and the D^0 decay time introduced by the selection requirements. The nuisance asymmetries are therefore removed by equalising the kinematics of tagging π^+ and π^- and of D^0 and \bar{D}^0 candidates, by weighting their kinematic distributions to their average. Figure 5 shows how the D^0 transverse momentum is correlated with the decay time and the effect of the weighting procedure to the time-dependent raw asymmetry. A side effect of the kinematic

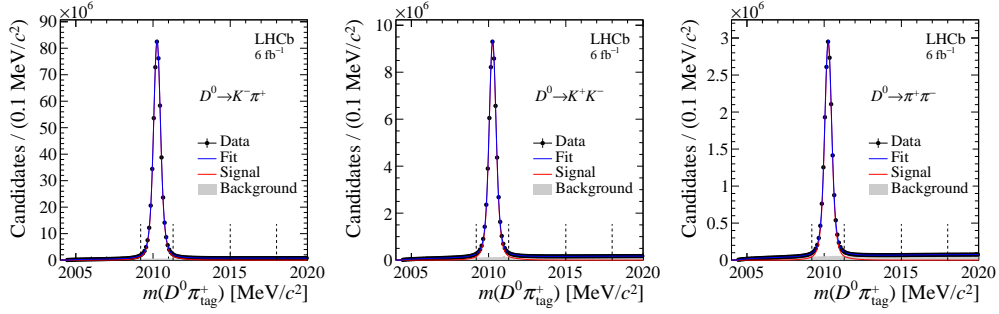


Figure 4: Distribution of $m(D^0\pi^+)$ for **(left)** $D^0 \rightarrow K^-\pi^+$, **(center)** $D^0 \rightarrow K^+K^-$ and **(right)** $D^0 \rightarrow \pi^+\pi^-$ candidates. The signal window and the lateral window used to remove the combinatorial background (grey filled area) are delimited by the vertical dashed lines. Fit projections are overlaid.

weighting is that, because of the correlation between the decay time and momentum of the D^0 meson, a possible time-dependent asymmetry due to a non-zero value of ΔY_f would be partially cancelled by the kinematic weighting, inducing a dilution in the measurement. By introducing different artificial values of $\Delta Y_{K^-\pi^+}$ in the $D^0 \rightarrow K^-\pi^+$ sample, up to values as large as 100 times the statistical uncertainty of the final measurement, the dilution is found to have a linear effect on the measured value of $\Delta Y_{K^-\pi^+}$ equal to $(96.9 \pm 0.1)\%$ of the introduced value. The results of all decay channels are therefore corrected to account for this dilution factor.

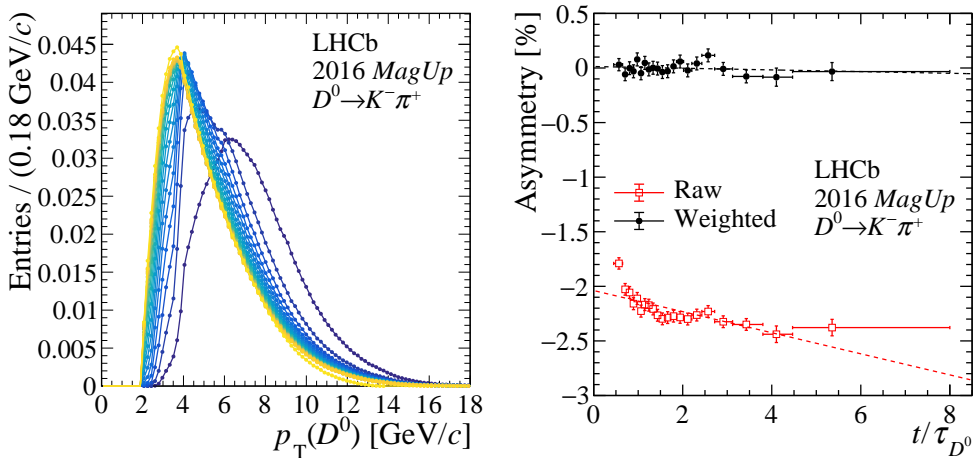


Figure 5: **(Left)** Normalised distributions of the D^0 transverse momentum, in different colours for each decay-time interval. Decay time increases from blue to yellow colour. **(Right)** Linear fit to the time-dependent asymmetry (red) before and (black) after the kinematic weighting. The plots correspond to the $D^0 \rightarrow K^-\pi^+$ candidates recorded in 2016 with the magnet polarity pointing upwards.

The presence of D^{*+} mesons originating from B mesons in the selected sample can potentially induce a bias in the measured time-dependent asymmetry, due to a difference in production asymmetry between D^{*+} mesons originating from secondary decays and D^{*+} mesons produced in pp collisions. In addition, the measurement of the decay time is performed with respect to the PV, resulting in a biased decay time towards larger

values for secondary D^{*+} mesons. Although the secondary decays are suppressed by a requirement on the IP of the D^0 meson, some contamination is still present in the sample. The size and asymmetry of this background is therefore assessed by means of a binned maximum-likelihood fit to the bidimensional distribution of IP and decay time of the $D^0 \rightarrow K^-\pi^+$ candidates, and the effect of secondary decays on the final measurement is corrected for. Systematic uncertainties are assessed related to background removal, mass difference between D^{*+} and D^{*-} , correction due to secondary decays, presence of misidentified background peaking in $m(D^0\pi^+)$ distribution and kinematic weighting.

The slope of the time-dependent asymmetry of the control sample is measured to be $(-0.4 \pm 0.5 \pm 0.2) \times 10^{-4}$, compatible with 0 as expected. The time-dependent asymmetries of the $D^0 \rightarrow K^+K^-$ and $D^0 \rightarrow \pi^+\pi^-$ channels, after the full selection, weighting and corrections, are displayed in Figure 6, with linear fits superimposed. The resulting slopes are

$$\begin{aligned}\Delta Y_{K^+K^-} &= (-2.3 \pm 1.5 \pm 0.3) \times 10^{-4}, \\ \Delta Y_{\pi^+\pi^-} &= (-4.0 \pm 2.8 \pm 0.4) \times 10^{-4},\end{aligned}$$

where the first uncertainties are statistical and the second are systematic, compatible with each other and with previous determinations. Assuming no final-state dependency, and taking account of the correlation between the systematic uncertainties, the combination of the two values gives

$$\Delta Y = (-2.7 \pm 1.3 \pm 0.3) \times 10^{-4},$$

consistent with zero within two standard deviations [80]. The combination with previous LHCb measurements [25, 26, 28] leads to

$$\begin{aligned}\Delta Y_{K^+K^-} &= (-0.3 \pm 1.3 \pm 0.3) \times 10^{-4}, \\ \Delta Y_{\pi^+\pi^-} &= (-3.6 \pm 2.4 \pm 0.4) \times 10^{-4}, \\ \Delta Y &= (-1.0 \pm 1.1 \pm 0.3) \times 10^{-4}.\end{aligned}$$

This result, consistent with no time-dependent CP violation, is the most precise measurement of CP violation in charm decays and improves by nearly a factor of two the precision of the previous world average of ΔY [79].

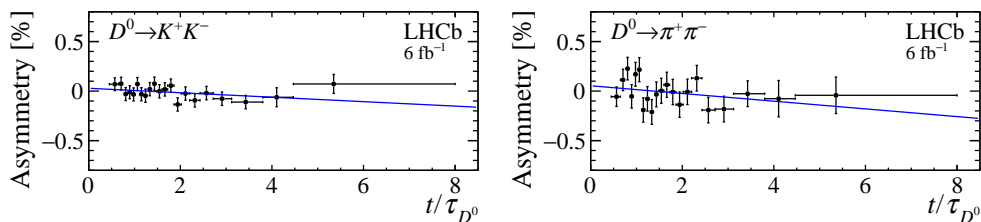


Figure 6: Asymmetry as a function of D^0 decay time, for (left) $D^0 \rightarrow K^+K^-$ and (right) $D^0 \rightarrow \pi^+\pi^-$ samples, with linear fit superimposed.

2.4 Observation of the mass difference between neutral charm-meson eigenstates

There are currently no precise SM estimates of the mixing parameters of the D^0 meson. The inclusive approach, that relies on the heavy-quark expansion, predicts a value of y in

large disagreement with experimental results [81–85]. The disagreement can be due to a violation of the quark-hadron duality or to a lifting of the GIM suppression for higher-dimension operators, even if these effects seem too small to explain the discrepancy [86–91]. The exclusive approach, which calculates the mixing amplitudes at the hadron level by summing the contributions of all possible intermediate virtual states, predicts the size of x and y to be $\mathcal{O}(10^{-3})$ [92–97].

According to the current world averages, the values of the mixing and CP -violating parameters of the D^0 meson are $x = (3.7 \pm 1.2) \times 10^{-3}$, $y = (6.8_{-0.7}^{+0.6}) \times 10^{-3}$, $|q/p| = (0.951_{-0.042}^{+0.053})$ and $\phi = (-0.092_{-0.079}^{+0.085})$ [79]. These parameters have been measured by studying mainly the $D^0 \rightarrow K^+\pi^-$ decay, that allowed precise determinations of y and the observation of mixing in the D^0 meson, and the $D^0 \rightarrow K_s^0\pi^+\pi^-$ decay, which is particularly sensitive to x [41, 98–101]. Here, the recent measurement of the mixing and CP violation parameters in $D^0 \rightarrow K_s^0\pi^+\pi^-$ decays performed by the LHCb collaboration with the data collected between 2016 and 2018, corresponding to 5.4 fb^{-1} of integrated luminosity, is summarised.

The analysis uses the “bin-flip” method [102], that consists in measuring, as a function of the D^0 decay time, the ratio of the number of decays between symmetric bins in the Dalitz plot defined by the two squared invariant masses $m^2(K_s^0\pi^\pm)$. The “bin-flip” method is a model-independent approach and does not require an accurate modelling of the efficiency. The Dalitz bins, illustrated in Figure 7, are defined in such a way that the strong-phase difference between the D^0 and \bar{D}^0 amplitudes within each bin is nearly constant [103]. The set of bins for which $m_+^2 > m_-^2$, where m_\pm^2 denotes $m^2(K_s^0\pi^\pm)$, is given a positive index $+b$, whereas the other set, symmetric about the $m_+^2 = m_-^2$ bisector, is given a negative index $-b$. For initially produced D^0 (\bar{D}^0) mesons, if the CP conserving amplitudes and mixing parameters are small, the expected ratios R_{bj}^+ (R_{bj}^-) of the number of decays in each negative Dalitz-plot bin ($-b$) to its positive counterpart ($+b$), for each decay-time interval j , is

$$R_{bj}^\pm \approx \frac{r_b + r_b \frac{\langle t^2 \rangle_j}{4} \text{Re}(z_{CP}^2 - \Delta z^2) + \frac{\langle t^2 \rangle_j}{4} |z_{CP} \pm \Delta z|^2 + \sqrt{r_b} \langle t \rangle_j \text{Re}[X_b^*(z_{CP} \pm \Delta z)]}{1 + \frac{\langle t^2 \rangle_j}{4} \text{Re}(z_{CP}^2 - \Delta z^2) + r_b \frac{\langle t^2 \rangle_j}{4} |z_{CP} \pm \Delta z|^2 + \sqrt{r_b} \langle t \rangle_j \text{Re}[X_b(z_{CP} \pm \Delta z)]}, \quad (12)$$

where r_b is the value of R_{bj}^\pm at decay time $t = 0$, X_b is the amplitude-weighted strong-phase difference between opposite bins and $\langle t \rangle_j$ ($\langle t^2 \rangle_j$) is the average (squared) decay time in each positive Dalitz-plot region in units of the D^0 lifetime. The other parameters are defined according to

$$z_{CP} \pm \Delta z \equiv - \left(\frac{q}{p} \right)^{\pm 1} (y + ix), \quad (13)$$

and are obtained from a simultaneous fit of the observed R_{bj}^\pm ratios, where external information on $c_b \equiv \text{Re}(X_b)$ and $s_b \equiv -\text{Im}(X_b)$ is used as a constraint [103, 104]. The CP -even mixing parameters x_{CP} and y_{CP} and the CP -violating parameters Δx and Δy

are therefore obtained

$$x_{CP} \equiv -\text{Im}(z_{CP}), \quad (14)$$

$$y_{CP} \equiv -\text{Re}(z_{CP}), \quad (15)$$

$$\Delta x \equiv -\text{Im}(\Delta z), \quad (16)$$

$$\Delta y \equiv -\text{Re}(\Delta z). \quad (17)$$

If CP is conserved, $x_{CP} = x$, $y_{CP} = y$ and $\Delta x = \Delta y = 0$.

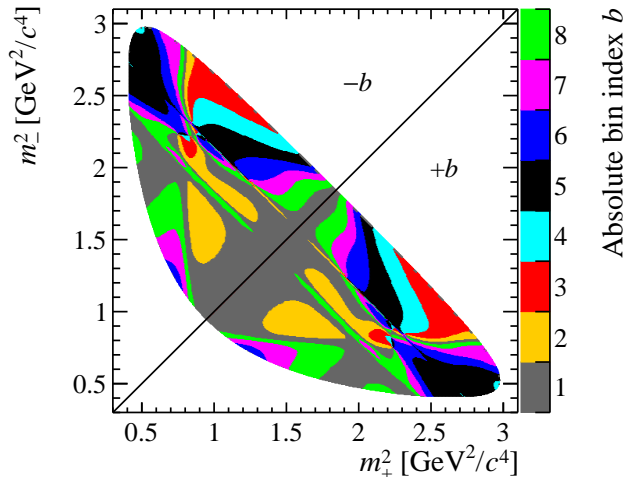


Figure 7: Binning scheme of the $D^0 \rightarrow K_s^0 \pi^+ \pi^-$ Dalitz plot.

The data sample is split in two categories depending on whether the K_s^0 meson is reconstructed using long or downstream pions, as already explained in Section 2.1. The flavour of the D^0 candidate is determined by the charge of the accompanying pion in the reconstructed $D^{*+} \rightarrow D^0 \pi^+$ decay. To determine the signal yields, a fit is performed on the invariant mass difference $\Delta m \equiv m(D^{*+}) - m(D^0)$ in each Dalitz-plot bin and decay-time interval, separately for D^0 flavour and K_s^0 category. The fit uses an empirical model that takes into account contributions from signal and combinatorial background. A total of about 31 million signal decays is found in the whole data sample.

The signal selection includes requirements on the displacement and momenta of the D^0 decay products that introduce efficiency variations correlated between the phase-space coordinates and the D^0 decay time, resulting in a possible bias on the measurement. A data-driven correction is therefore applied to make the decay-time acceptance uniform in the phase space, removing the correlation. A further correction is performed to cancel detection asymmetries of the pions produced in the D^0 decays, since their kinematics depend on the Dalitz-plot coordinate and the D^0 flavour: the two-track $\pi^+ \pi^-$ detection asymmetry is evaluated by measuring the raw asymmetries in the control samples $D_s^+ \rightarrow \pi^+ \pi^+ \pi^-$ and $D_s^+ \rightarrow \phi \pi^+$ in each Dalitz-plot bin, after weighting their kinematics to that of the signal sample.

A fit is performed on all the corrected R_{bj}^\pm ratios to determine the mixing and CP violating parameters. The result is illustrated in Figure 8. Various sources of systematic uncertainties are considered and assessed from ensembles of pseudoexperiments. They

take into account contributions related to reconstruction and selection effects, decay-time and m_{\pm} resolution, presence of secondary D^{*+} decays, $\pi^+\pi^-$ detection asymmetry, fit model and approximation of strong phase input to be constant in each bin. The mixing and CP violation parameters are measured to be

$$\begin{aligned} x_{CP} &= (3.97 \pm 0.46 \pm 0.29) \times 10^{-3}, \\ y_{CP} &= (4.59 \pm 1.20 \pm 0.85) \times 10^{-3}, \\ \Delta x &= (-0.27 \pm 0.18 \pm 0.01) \times 10^{-3}, \\ \Delta y &= (0.20 \pm 0.36 \pm 0.13) \times 10^{-3}, \end{aligned}$$

where the first uncertainties are statistical and the second systematic [105].

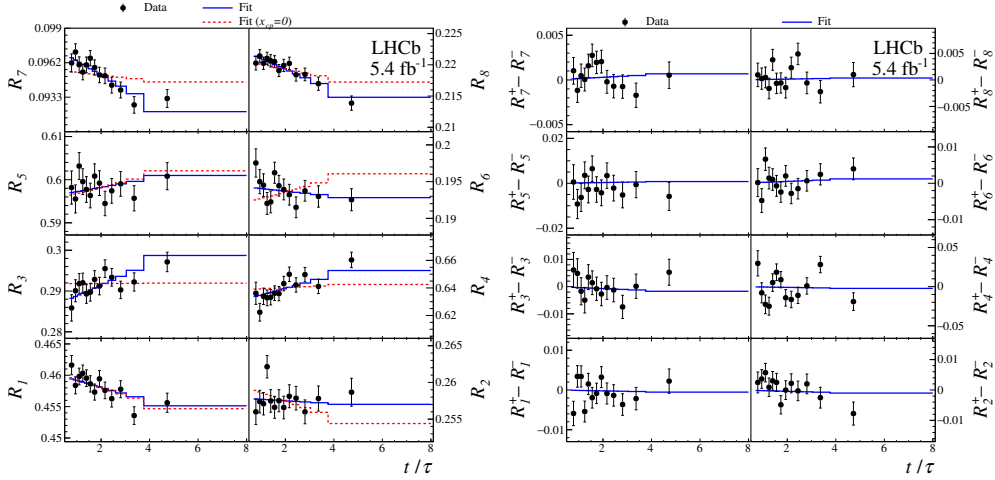


Figure 8: **(Left)** CP -averaged yield ratios and **(right)** differences of D^0 and \bar{D}^0 yield ratios as a function of D^0 decay time, shown for each Dalitz-plot bin. Fit projections are overlaid.

A likelihood function of x , y , $|q/p|$ and ϕ is built from the results using a likelihood-ratio ordering that assumes the observed correlations to be independent of the true parameter values [106], whose best fit point is

$$\begin{aligned} x &= (3.98^{+0.56}_{-0.54}) \times 10^{-3}, \\ y &= (4.6^{+1.5}_{-1.4}) \times 10^{-3}, \\ |q/p| &= 0.996 \pm 0.052, \\ \phi &= 0.056^{+0.047}_{-0.051}. \end{aligned}$$

This result corresponds to the first observation of a non-zero value of the mass difference x of neutral charm meson mass eigenstates with a significance of more than seven standard deviations. This measurement significantly improves limits on CP violation in mixing in the charm sector.

3 Conclusions and future prospects

The most recent results from LHCb concerning CP violation in charm sector have been summarised here. The analysis of data collected during the LHC Run 2 allowed the

most precise measurement of time-dependent CP asymmetry in D^0 decays to date to be obtained and a non-zero mass difference between neutral charm-meson eigenstates to be observed. Furthermore, the most precise measurement of CP asymmetry in $D^0 \rightarrow K_s^0 K_s^0$ decays has been performed. CP asymmetries in two-body decays of charged charm mesons in final states with light neutral mesons have been determined with precisions of the order of 10^{-2} . Many key measurements are still to be performed with the full data sets collected by LHCb, such as the determination of $\mathcal{A}_{CP}(D^0 \rightarrow K^+ K^-)$, which is expected to be measured with an uncertainty of the order of 7×10^{-4} , and of $y_{CP}^{h^+ h^-}$, defined as the deviation from unity of the average of the effective decay widths of $D^0 \rightarrow h^+ h^-$ and $\bar{D}^0 \rightarrow h^+ h^-$ decays.

Starting from 2022, the Upgrade I of the LHCb experiment will increase the total integrated luminosity to 23 fb^{-1} (50 fb^{-1}) by the end of its third (fourth) data-taking period [107, 108]. An Upgrade II of the LHCb experiment was recently proposed and, if approved, it will allow the total integrated luminosity to be increased to 300 fb^{-1} [109]. With such a large data set, the statistical uncertainty of ΔY will be reduced to a value below 2×10^{-5} , and that of $\mathcal{A}_{CP}(D^0 \rightarrow K^+ K^-)$ will become smaller than 10^{-4} [110]. The statistical uncertainty of the mixing parameters measured with the $D^0 \rightarrow K_s^0 \pi^+ \pi^-$ decay mode is expected to decrease by an order of magnitude. For what concerns the CP asymmetry of the $D^0 \rightarrow K_s^0 K_s^0$ decay, its projected statistical uncertainty is expected to decrease by a factor 4, reaching $\mathcal{O}(10^{-3})$. For all the mentioned decay modes, there are no systematic uncertainties that are known to have irreducible contributions which exceed the ultimate statistical precision. The LHCb Upgrade I and II will therefore have a strong potential of probing the Standard Model contribution and an impressive power to characterise new physics contributions to CP violation in the charm sector.

References

- [1] Y. Grossman, Y. Nir, and G. Perez, “Testing New Indirect CP Violation,” *Phys. Rev. Lett.*, vol. 103, p. 071602, 2009.
- [2] A. L. Kagan and M. D. Sokoloff, “On Indirect CP Violation and Implications for $D^0 - \bar{D}^0$ and $B_{(s)} - \bar{B}_{(s)}$ mixing,” *Phys. Rev. D*, vol. 80, p. 076008, 2009.
- [3] M. Golden and B. Grinstein, “Enhanced CP Violations in Hadronic Charm Decays,” *Phys. Lett. B*, vol. 222, pp. 501–506, 1989.
- [4] F. Buccella, M. Lusignoli, G. Miele, A. Pugliese, and P. Santorelli, “Nonleptonic weak decays of charmed mesons,” *Phys. Rev. D*, vol. 51, pp. 3478–3486, 1995.
- [5] S. Bianco, F. L. Fabbri, D. Benson, and I. Bigi, “A Cicerone for the physics of charm,” *Riv. Nuovo Cim.*, vol. 26, no. 7-8, pp. 1–200, 2003.
- [6] M. Artuso, B. Meadows, and A. A. Petrov, “Charm Meson Decays,” *Ann. Rev. Nucl. Part. Sci.*, vol. 58, pp. 249–291, 2008.
- [7] J. Brod, A. L. Kagan, and J. Zupan, “Size of direct CP violation in singly Cabibbo-suppressed D decays,” *Phys. Rev. D*, vol. 86, p. 014023, 2012.

- [8] H.-Y. Cheng and C.-W. Chiang, “Direct CP violation in two-body hadronic charmed meson decays,” *Phys. Rev. D*, vol. 85, p. 034036, 2012. [Erratum: *Phys.Rev.D* 85, 079903 (2012)].
- [9] H.-Y. Cheng and C.-W. Chiang, “SU(3) symmetry breaking and CP violation in $D \rightarrow PP$ decays,” *Phys. Rev. D*, vol. 86, p. 014014, 2012.
- [10] H.-n. Li, C.-D. Lu, and F.-S. Yu, “Branching ratios and direct CP asymmetries in $D \rightarrow PP$ decays,” *Phys. Rev. D*, vol. 86, p. 036012, 2012.
- [11] E. Franco, S. Mishima, and L. Silvestrini, “The Standard Model confronts CP violation in $D^0 \rightarrow \pi^+\pi^-$ and $D^0 \rightarrow K^+K^-$,” *JHEP*, vol. 05, p. 140, 2012.
- [12] D. Pirtskhalava and P. Uttayarat, “ CP Violation and Flavor SU(3) Breaking in D-meson Decays,” *Phys. Lett. B*, vol. 712, pp. 81–86, 2012.
- [13] T. Feldmann, S. Nandi, and A. Soni, “Repercussions of Flavour Symmetry Breaking on CP Violation in D -Meson Decays,” *JHEP*, vol. 06, p. 007, 2012.
- [14] J. Brod, Y. Grossman, A. L. Kagan, and J. Zupan, “A Consistent Picture for Large Penguins in $D \rightarrow \pi^+\pi^-, K^+K^-$,” *JHEP*, vol. 10, p. 161, 2012.
- [15] G. Hiller, M. Jung, and S. Schacht, “SU(3)-flavor anatomy of nonleptonic charm decays,” *Phys. Rev. D*, vol. 87, no. 1, p. 014024, 2013.
- [16] Y. Grossman and D. J. Robinson, “SU(3) Sum Rules for Charm Decay,” *JHEP*, vol. 04, p. 067, 2013.
- [17] B. Bhattacharya, M. Gronau, and J. L. Rosner, “ CP asymmetries in singly-Cabibbo-suppressed D decays to two pseudoscalar mesons,” *Phys. Rev. D*, vol. 85, p. 054014, 2012.
- [18] S. Müller, U. Nierste, and S. Schacht, “Sum Rules of Charm CP Asymmetries beyond the SU(3) $_F$ Limit,” *Phys. Rev. Lett.*, vol. 115, no. 25, p. 251802, 2015.
- [19] A. Khodjamirian and A. A. Petrov, “Direct CP asymmetry in $D \rightarrow \pi^-\pi^+$ and $D \rightarrow K^-K^+$ in QCD-based approach,” *Phys. Lett. B*, vol. 774, pp. 235–242, 2017.
- [20] F. Buccella, A. Paul, and P. Santorelli, “SU(3) $_F$ breaking through final state interactions and CP asymmetries in $D \rightarrow PP$ decays,” *Phys. Rev. D*, vol. 99, no. 11, p. 113001, 2019.
- [21] R. Aaij *et al.*, “Measurements of prompt charm production cross-sections in pp collisions at $\sqrt{s} = 13$ TeV,” *JHEP*, vol. 03, p. 159, 2016. [Erratum: *JHEP* 09, 013 (2016), Erratum: *JHEP* 05, 074 (2017)].
- [22] R. Aaij *et al.*, “Search for CP violation in $D^\pm \rightarrow K_S^0 K^\pm$ and $D_s^\pm \rightarrow K_S^0 \pi^\pm$ decays,” *JHEP*, vol. 10, p. 025, 2014.
- [23] R. Aaij *et al.*, “Measurement of CP asymmetries in $D^\pm \rightarrow \eta' \pi^\pm$ and $D_s^\pm \rightarrow \eta' \pi^\pm$ decays,” *Phys. Lett. B*, vol. 771, pp. 21–30, 2017.

- [24] R. Aaij *et al.*, “Search for CP violation in $D_s^+ \rightarrow K_S^0\pi^+$, $D^+ \rightarrow K_S^0K^+$ and $D^+ \rightarrow \phi\pi^+$ decays,” *Phys. Rev. Lett.*, vol. 122, no. 19, p. 191803, 2019.
- [25] R. Aaij *et al.*, “Measurement of indirect CP asymmetries in $D^0 \rightarrow K^-K^+$ and $D^0 \rightarrow \pi^-\pi^+$ decays using semileptonic B decays,” *JHEP*, vol. 04, p. 043, 2015.
- [26] R. Aaij *et al.*, “Measurement of the CP violation parameter A_Γ in $D^0 \rightarrow K^+K^-$ and $D^0 \rightarrow \pi^+\pi^-$ decays,” *Phys. Rev. Lett.*, vol. 118, no. 26, p. 261803, 2017.
- [27] R. Aaij *et al.*, “Measurement of the Charm-Mixing Parameter y_{CP} ,” *Phys. Rev. Lett.*, vol. 122, no. 1, p. 011802, 2019.
- [28] R. Aaij *et al.*, “Updated measurement of decay-time-dependent CP asymmetries in $D^0 \rightarrow K^+K^-$ and $D^0 \rightarrow \pi^+\pi^-$ decays,” *Phys. Rev. D*, vol. 101, no. 1, p. 012005, 2020.
- [29] R. Aaij *et al.*, “Measurement of CP asymmetry in $D^0 \rightarrow K^-K^+$ and $D^0 \rightarrow \pi^-\pi^+$ decays,” *JHEP*, vol. 07, p. 041, 2014.
- [30] R. Aaij *et al.*, “Measurement of the difference of time-integrated CP asymmetries in $D^0 \rightarrow K^-K^+$ and $D^0 \rightarrow \pi^-\pi^+$ decays,” *Phys. Rev. Lett.*, vol. 116, no. 19, p. 191601, 2016.
- [31] R. Aaij *et al.*, “Measurement of CP asymmetry in $D^0 \rightarrow K^-K^+$ decays,” *Phys. Lett. B*, vol. 767, pp. 177–187, 2017.
- [32] R. Aaij *et al.*, “Measurements of charm mixing and CP violation using $D^0 \rightarrow K^\pm\pi^\mp$ decays,” *Phys. Rev. D*, vol. 95, no. 5, p. 052004, 2017. [Erratum: *Phys.Rev.D* 96, 099907 (2017)].
- [33] R. Aaij *et al.*, “Updated determination of D^0 - \bar{D}^0 mixing and CP violation parameters with $D^0 \rightarrow K^+\pi^-$ decays,” *Phys. Rev. D*, vol. 97, no. 3, p. 031101, 2018.
- [34] R. Aaij *et al.*, “Model-independent search for CP violation in $D^0 \rightarrow K^-K^+\pi^-\pi^+$ and $D^0 \rightarrow \pi^-\pi^+\pi^+\pi^-$ decays,” *Phys. Lett. B*, vol. 726, pp. 623–633, 2013.
- [35] R. Aaij *et al.*, “Search for CP violation in the decay $D^+ \rightarrow \pi^-\pi^+\pi^+$,” *Phys. Lett. B*, vol. 728, pp. 585–595, 2014.
- [36] R. Aaij *et al.*, “Search for CP violation using T -odd correlations in $D^0 \rightarrow K^+K^-\pi^+\pi^-$ decays,” *JHEP*, vol. 10, p. 005, 2014.
- [37] R. Aaij *et al.*, “Search for CP violation in $D^0 \rightarrow \pi^-\pi^+\pi^0$ decays with the energy test,” *Phys. Lett. B*, vol. 740, pp. 158–167, 2015.
- [38] R. Aaij *et al.*, “Measurement of Angular and CP Asymmetries in $D^0 \rightarrow \pi^+\pi^-\mu^+\mu^-$ and $D^0 \rightarrow K^+K^-\mu^+\mu^-$ decays,” *Phys. Rev. Lett.*, vol. 121, no. 9, p. 091801, 2018.
- [39] R. Aaij *et al.*, “Search for CP violation through an amplitude analysis of $D^0 \rightarrow K^+K^-\pi^+\pi^-$ decays,” *JHEP*, vol. 02, p. 126, 2019.
- [40] R. Aaij *et al.*, “Measurement of the time-integrated CP asymmetry in $D^0 \rightarrow K_S^0K_S^0$ decays,” *JHEP*, vol. 11, p. 048, 2018.

- [41] R. Aaij *et al.*, “Measurement of the mass difference between neutral charm-meson eigenstates,” *Phys. Rev. Lett.*, vol. 122, no. 23, p. 231802, 2019.
- [42] R. Aaij *et al.*, “A measurement of the CP asymmetry difference in $\Lambda_c^+ \rightarrow pK^-K^+$ and $p\pi^-\pi^+$ decays,” *JHEP*, vol. 03, p. 182, 2018.
- [43] R. Aaij *et al.*, “Search for CP violation in $\Xi_c^+ \rightarrow pK^-\pi^+$ decays using model-independent techniques,” *Eur. Phys. J. C*, vol. 80, no. 10, p. 986, 2020.
- [44] R. Aaij *et al.*, “Observation of CP Violation in Charm Decays,” *Phys. Rev. Lett.*, vol. 122, no. 21, p. 211803, 2019.
- [45] Y. Grossman, A. L. Kagan, and Y. Nir, “New physics and CP violation in singly Cabibbo suppressed D decays,” *Phys. Rev. D*, vol. 75, p. 036008, 2007.
- [46] M. Chala, A. Lenz, A. V. Rusov, and J. Scholtz, “ ΔA_{CP} within the Standard Model and beyond,” *JHEP*, vol. 07, p. 161, 2019.
- [47] Y. Grossman and S. Schacht, “The emergence of the $\Delta U = 0$ rule in charm physics,” *JHEP*, vol. 07, p. 020, 2019.
- [48] H.-N. Li, C.-D. Lu, and F.-S. Yu, “Implications on the first observation of charm CPV at LHCb,” 3 2019.
- [49] A. Soni, “Resonance enhancement of Charm CP ,” 5 2019.
- [50] H.-Y. Cheng and C.-W. Chiang, “Revisiting CP violation in $D \rightarrow PP$ and VP decays,” *Phys. Rev. D*, vol. 100, no. 9, p. 093002, 2019.
- [51] A. Dery and Y. Nir, “Implications of the LHCb discovery of CP violation in charm decays,” *JHEP*, vol. 12, p. 104, 2019.
- [52] D. Wang, C.-P. Jia, and F.-S. Yu, “A self-consistent framework of topological amplitude and its $SU(N)$ decomposition,” 1 2020.
- [53] R. Bause, H. Gisbert, M. Golz, and G. Hiller, “Exploiting CP -asymmetries in rare charm decays,” *Phys. Rev. D*, vol. 101, no. 11, p. 115006, 2020.
- [54] A. Dery, Y. Grossman, S. Schacht, and A. Soffer, “Probing the $\Delta U = 0$ rule in three body charm decays,” *JHEP*, vol. 05, p. 179, 2021.
- [55] H.-Y. Cheng and C.-W. Chiang, “ CP violation in quasi-two-body $D \rightarrow VP$ decays and three-body D decays mediated by vector resonances,” 4 2021.
- [56] A. L. Kagan and L. Silvestrini, “Dispersive and absorptive CP violation in $D^0 - \overline{D}^0$ mixing,” *Phys. Rev. D*, vol. 103, no. 5, p. 053008, 2021.
- [57] A. A. Alves, Jr. *et al.*, “The LHCb Detector at the LHC,” *JINST*, vol. 3, p. S08005, 2008.
- [58] R. Aaij *et al.*, “LHCb Detector Performance,” *Int. J. Mod. Phys. A*, vol. 30, no. 07, p. 1530022, 2015.

- [59] R. Aaij *et al.*, “Measurement of B^0 , B_s^0 , B^+ and Λ_b^0 production asymmetries in 7 and 8 TeV proton-proton collisions,” *Phys. Lett. B*, vol. 774, pp. 139–158, 2017.
- [60] R. Aaij *et al.*, “Measurement of the flavour-specific CP -violating asymmetry a_{sl}^s in B_s^0 decays,” *Phys. Lett. B*, vol. 728, pp. 607–615, 2014.
- [61] R. Aaij *et al.*, “Measurement of the D^\pm production asymmetry in 7 TeV pp collisions,” *Phys. Lett. B*, vol. 718, pp. 902–909, 2013.
- [62] R. Aaij *et al.*, “Measurement of the $D_s^+ - D_s^-$ production asymmetry in 7 TeV pp collisions,” *Phys. Lett. B*, vol. 713, pp. 186–195, 2012.
- [63] U. Nierste and S. Schacht, “ CP Violation in $D^0 \rightarrow K_S K_S$,” *Phys. Rev. D*, vol. 92, no. 5, p. 054036, 2015.
- [64] G. Bonvicini *et al.*, “Search for CP violation in $D^0 \rightarrow K_S^0 \pi^0$ and $D^0 \rightarrow \pi^0 \pi^0$ and $D^0 \rightarrow K_S^0 K_S^0$ decays,” *Phys. Rev. D*, vol. 63, p. 071101, 2001.
- [65] N. Dash *et al.*, “Search for CP Violation and Measurement of the Branching Fraction in the Decay $D^0 \rightarrow K_S^0 K_S^0$,” *Phys. Rev. Lett.*, vol. 119, no. 17, p. 171801, 2017.
- [66] R. Aaij *et al.*, “Measurement of the time-integrated CP asymmetry in $D^0 \rightarrow K_S^0 K_S^0$ decays,” *JHEP*, vol. 10, p. 055, 2015.
- [67] R. Aaij *et al.*, “Measurement of CP asymmetry in $D^0 \rightarrow K_S^0 K_S^0$ decays,” 5 2021.
- [68] V. Babu *et al.*, “Search for CP violation in the $D^+ \rightarrow \pi^+ \pi^0$ decay at Belle,” *Phys. Rev. D*, vol. 97, no. 1, p. 011101, 2018.
- [69] Y. Guan *et al.*, “Measurement of branching fractions and CP asymmetries for $D_s^+ \rightarrow K^+(\eta, \pi^0)$ and $D_s^+ \rightarrow \pi^+(\eta, \pi^0)$ decays at Belle,” *Phys. Rev. D*, vol. 103, p. 112005, 2021.
- [70] P. A. Zyla *et al.*, “Review of Particle Physics,” *PTEP*, vol. 2020, no. 8, p. 083C01, 2020.
- [71] R. Aaij *et al.*, “Search for CP violation in $D_{(s)}^+ \rightarrow h^+ \pi^0$ and $D_{(s)}^+ \rightarrow h^+ \eta$ decays,” *JHEP*, vol. 06, p. 019, 2021.
- [72] H. Mendez *et al.*, “Measurements of D Meson Decays to Two Pseudoscalar Mesons,” *Phys. Rev. D*, vol. 81, p. 052013, 2010.
- [73] H.-N. Li, H. Umeeda, F. Xu, and F.-S. Yu, “ D meson mixing as an inverse problem,” *Phys. Lett. B*, vol. 810, p. 135802, 2020.
- [74] T. Pajero and M. J. Morello, “Mixing and CP violation in $D \rightarrow K^- \pi^+$ decays,” 6 2021.
- [75] T. Pajero, *Search for time-dependent CP violation in $D^0 \rightarrow K^+ K^-$ and $D^0 \rightarrow \pi^+ \pi^-$ decays*. PhD thesis, Pisa, Scuola Normale Superiore, 2021.
- [76] J. P. Lees *et al.*, “Measurement of $D^0 - \bar{D}^0$ Mixing and CP Violation in Two-Body D^0 Decays,” *Phys. Rev. D*, vol. 87, no. 1, p. 012004, 2013.

- [77] T. A. Aaltonen *et al.*, “Measurement of indirect CP -violating asymmetries in $D^0 \rightarrow K^+K^-$ and $D^0 \rightarrow \pi^+\pi^-$ decays at CDF,” *Phys. Rev. D*, vol. 90, no. 11, p. 111103, 2014.
- [78] M. Starič *et al.*, “Measurement of $D^0 - \bar{D}^0$ mixing and search for CP violation in $D^0 \rightarrow K^+K^-, \pi^+\pi^-$ decays with the full Belle data set,” *Phys. Lett. B*, vol. 753, pp. 412–418, 2016.
- [79] Y. S. Amhis *et al.*, “Averages of b -hadron, c -hadron, and τ -lepton properties as of 2018,” *Eur. Phys. J. C*, vol. 81, no. 3, p. 226, 2021.
- [80] R. Aaij *et al.*, “Search for time-dependent CP violation in $D^0 \rightarrow K^+K^-$ and $D^0 \rightarrow \pi^+\pi^-$ decays,” 5 2021.
- [81] N. Carrasco *et al.*, “ $D^0 - \bar{D}^0$ mixing in the standard model and beyond from $N_f = 2$ twisted mass QCD,” *Phys. Rev. D*, vol. 90, no. 1, p. 014502, 2014.
- [82] M. Kirk, A. Lenz, and T. Rauh, “Dimension-six matrix elements for meson mixing and lifetimes from sum rules,” *JHEP*, vol. 12, p. 068, 2017. [Erratum: *JHEP* 06, 162 (2020)].
- [83] N. Carrasco, P. Dimopoulos, R. Frezzotti, V. Lubicz, G. C. Rossi, S. Simula, and C. Tarantino, “ $\Delta S=2$ and $\Delta C=2$ bag parameters in the standard model and beyond from $N_f=2+1+1$ twisted-mass lattice QCD,” *Phys. Rev. D*, vol. 92, no. 3, p. 034516, 2015.
- [84] A. Bazavov *et al.*, “Short-distance matrix elements for D^0 -meson mixing for $N_f = 2 + 1$ lattice QCD,” *Phys. Rev. D*, vol. 97, no. 3, p. 034513, 2018.
- [85] A. Lenz, M. L. Piscopo, and C. Vlahos, “Renormalization scale setting for D -meson mixing,” *Phys. Rev. D*, vol. 102, no. 9, p. 093002, 2020.
- [86] T. Jubb, M. Kirk, A. Lenz, and G. Tetlalmatzi-Xolocotzi, “On the ultimate precision of meson mixing observables,” *Nucl. Phys. B*, vol. 915, pp. 431–453, 2017.
- [87] H. Georgi, “ D - anti- D mixing in heavy quark effective field theory,” *Phys. Lett. B*, vol. 297, pp. 353–357, 1992.
- [88] T. Ohl, G. Ricciardi, and E. H. Simmons, “ D - anti- D mixing in heavy quark effective field theory: The Sequel,” *Nucl. Phys. B*, vol. 403, pp. 605–632, 1993.
- [89] I. I. Y. Bigi and N. G. Uraltsev, “ D^0 - anti- D^0 oscillations as a probe of quark hadron duality,” *Nucl. Phys. B*, vol. 592, pp. 92–106, 2001.
- [90] M. Bobrowski, A. Lenz, J. Riedl, and J. Rohrwild, “How Large Can the SM Contribution to CP Violation in $D^0 - \bar{D}^0$ Mixing Be?,” *JHEP*, vol. 03, p. 009, 2010.
- [91] M. Bobrowski, A. Lenz, and T. Rauh, “Short distance D - \bar{D} mixing,” in *5th International Workshop on Charm Physics*, 8 2012.
- [92] A. F. Falk, Y. Grossman, Z. Ligeti, and A. A. Petrov, “ $SU(3)$ breaking and D^0 - anti- D^0 mixing,” *Phys. Rev. D*, vol. 65, p. 054034, 2002.

- [93] M. Gronau and J. L. Rosner, “Revisiting D^0 - D^0 bar mixing using U-spin,” *Phys. Rev. D*, vol. 86, p. 114029, 2012.
- [94] H.-Y. Cheng and C.-W. Chiang, “Long-Distance Contributions to $D^0 - \bar{D}^0$ Mixing Parameters,” *Phys. Rev. D*, vol. 81, p. 114020, 2010.
- [95] H.-Y. Jiang, F.-S. Yu, Q. Qin, H.-n. Li, and C.-D. Lü, “ D^0 - \bar{D}^0 mixing parameter y in the factorization-assisted topological-amplitude approach,” *Chin. Phys. C*, vol. 42, no. 6, p. 063101, 2018.
- [96] L. Wolfenstein, “ D^0 anti- D^0 Mixing,” *Phys. Lett. B*, vol. 164, pp. 170–172, 1985.
- [97] J. F. Donoghue, E. Golowich, B. R. Holstein, and J. Trampetic, “Dispersive Effects in D^0 anti- D^0 Mixing,” *Phys. Rev. D*, vol. 33, p. 179, 1986.
- [98] D. M. Asner *et al.*, “Search for $D^0 - \bar{D}^0$ mixing in the Dalitz plot analysis of $D^0 \rightarrow K_s^0 \pi^+ \pi^-$,” *Phys. Rev. D*, vol. 72, p. 012001, 2005.
- [99] P. del Amo Sanchez *et al.*, “Measurement of $D^0 - \bar{D}^0$ mixing parameters using $D^0 \rightarrow K_s^0 \pi^+ \pi^-$ and $D^0 \rightarrow K_s^0 K^+ K^-$ decays,” *Phys. Rev. Lett.*, vol. 105, p. 081803, 2010.
- [100] T. Peng *et al.*, “Measurement of $D^0 - \bar{D}^0$ mixing and search for indirect CP violation using $D^0 \rightarrow K_s^0 \pi^+ \pi^-$ decays,” *Phys. Rev. D*, vol. 89, no. 9, p. 091103, 2014.
- [101] R. Aaij *et al.*, “Model-independent measurement of mixing parameters in $D^0 \rightarrow K_s^0 \pi^+ \pi^-$ decays,” *JHEP*, vol. 04, p. 033, 2016.
- [102] A. Di Canto, J. Garra Ticó, T. Gershon, N. Jurik, M. Martinelli, T. Pilař, S. Stahl, and D. Tonelli, “Novel method for measuring charm-mixing parameters using multibody decays,” *Phys. Rev. D*, vol. 99, no. 1, p. 012007, 2019.
- [103] J. Libby *et al.*, “Model-independent determination of the strong-phase difference between D^0 and $\bar{D}^0 \rightarrow K_{S,L}^0 h^+ h^-$ ($h = \pi, K$) and its impact on the measurement of the CKM angle γ/ϕ_3 ,” *Phys. Rev. D*, vol. 82, p. 112006, 2010.
- [104] M. Ablikim *et al.*, “Model-independent determination of the relative strong-phase difference between D^0 and $\bar{D}^0 \rightarrow K_{S,L}^0 \pi^+ \pi^-$ and its impact on the measurement of the CKM angle γ/ϕ_3 ,” *Phys. Rev. D*, vol. 101, no. 11, p. 112002, 2020.
- [105] R. Aaij *et al.*, “Observation of the mass difference between neutral charm-meson eigenstates,” 6 2021.
- [106] R. Aaij *et al.*, “Measurement of the CKM angle γ from a combination of $B^\pm \rightarrow Dh^\pm$ analyses,” *Phys. Lett. B*, vol. 726, pp. 151–163, 2013.
- [107] I. Bediaga *et al.*, “Framework TDR for the LHCb Upgrade: Technical Design Report,” 4 2012.
- [108] “LHCb Trigger and Online Upgrade Technical Design Report,” 5 2014.

- [109] R. Aaij *et al.*, “Expression of Interest for a Phase-II LHCb Upgrade: Opportunities in flavour physics, and beyond, in the HL-LHC era,” Feb 2017.
- [110] R. Aaij *et al.*, “Physics case for an LHCb Upgrade II - Opportunities in flavour physics, and beyond, in the HL-LHC era,” 8 2018.